A Continuous Comparison Radiometer at 97 GHz

C. READ PREDMORE, MEMBER, IEEE, NEAL R. ERICKSON, G. RICHARD HUGUENIN, MEMBER, IEEE, AND PAUL F. GOLDSMITH, MEMBER, IEEE

Abstract—**A continuous comparison radiometer has been implemented at 97 GHz using quasi-optical techniques for local oscillator (LO) injection and realization of a 90° hybrid. Cryogenically cooled Schottky-diode mixers and FET amplifiers give a double-sideband (DSB) system temperature of 250 K. The system is self-calibrating and optimized under computer control. The root-mean-square (rms) fluctuations due to the receiver are less than 0.025 K with a 1-s integration time.**

I. Introduction

A HIGH-SENSITIVITY, continuous comparison radiometer has been implemented by the Five College Radio Astronomy Observatory. The continuous comparison or correlation radiometer circuit is over twenty years old [1] and has been used for radio astronomical observations at 74 cm [2], 11 cm [3], and 6 cm [4]. Its use at millimeter wavelengths has been precluded due to the losses and imperfections in the available waveguide components. The extensive use of quasi-optical techniques for beam guidance, local oscillator (LO) injections, and a combination of the two beams in an input hybrid has resulted in major performance gains for the system described here.

The classical problem in radiometry is to distinguish a weak source in the presence of the much greater noise from the receiver and atmosphere and in the presence of fluctuations in receiver gain and atmospheric emission. For an astronomical object such as a quasar, this is accomplished by actually moving the telescope between the source position and an adjacent position at the same elevation at a 0.05–0.10-Hz rate, deflecting the beam by nutating the subreflector at a 0.5–5-Hz rate [5], Dicke switching [6] against a load, or deflecting the beam near the Cassegrain focal plane with a rotating beam chopper at up to 50 Hz [7].

In contrast, the continuous comparison radiometer has no moving parts for switching, so that the complexities of mechanical switching systems mentioned above, and the significant loss and mismatch of a ferrite switch, are avoided. Rather, two beams are continually subtracted to give the desired difference signal with an equivalent time constant which can be short as the reciprocal of the intermediate frequency (IF) bandwidth. Since the subtraction is performed continuously, fluctuations with very short time scales that are common to both beams are cancelled perfectly. In addition, the subtraction in the radiometer is insensitive to receiver gain changes.

The present system employs a LO frequency of 97 GHz and is sensitive to input signals in both sidebands with a separation from the LO of 4.4 to 5.0 GHz. The radiometer consists of a calibration system, cryogenic front end, and IF and signal processing units. The entire system is automatically optimized, calibrated, and operated by a computer. The root-mean-square (rms) sensitivity due to the receiver is less than 0.025 K with a 1-s integration time.

II. Basic Theory

The radiometer block diagram is shown in Fig. 1. The two input beams with temperature T_A and T_B as well as the 97.3-GHz LO are split by a quasi-optical 90° hybrid and double-sideband (DSB) mixed to 4.7 GHz. At 4.7 GHz, the voltages in the two IF amplifiers are proportional to $A - jB$ and $A + jB$, where A and B are the voltages of the inputs to the Dewar. The second frequency conversion is from 4.7 to 2.1 GHz using a 6.8-GHz LO. One of the LO lines has a 6-bit computer-controlled phase shifter with a 5.6° resolution to optimize the system sensitivity. Also under computer control are 0–50-dB p-i-n attenuators in each of the 2.1-GHz IF chains. Precision IF 180° hybrid, matched detectors, and an instrumentation operational amplifier are used to multiply the two IF signals.

The resultant response of the system is

$$V_{\mathrm{DIFF}} = C_{\mathrm{DIFF}}(T_A - T_B)\cos\phi \tag{1}$$

where C_{DIFF} is a calibration constant and ϕ is the phase of the LO phase shifter. Thus, the system is insensitive to gain fluctuations and is responsive only to the input temperature difference. A manual delay line with a 0.2-ns range is used to compensate for phase slopes in the cabling and amplifiers. The entire system is automatically optimized and calibrated with a ModComp MODACS computer.

Faris [1] has done an extensive analysis of correlation radiometers including the effects of nonidentical amplifiers, gain fluctuations, and differential phase and delay. Here, the system response will be analyzed for a single IF frequency to investigate the effect of amplitude imbalance in the input 90° hybrid and imperfect balance in the final IF detectors.

Manuscript received December 19, 1983; revised August 2, 1984. This work was supported in part by the M.I.T. Lincoln Laboratory under Contract F19628-80-C-0002.

The authors are with the Five College Radio Astronomy Observatory, University of Massachusetts, Amherst, MA 01003.

0018-9480/85/0100-0044$01.00 ©1984 IEEE

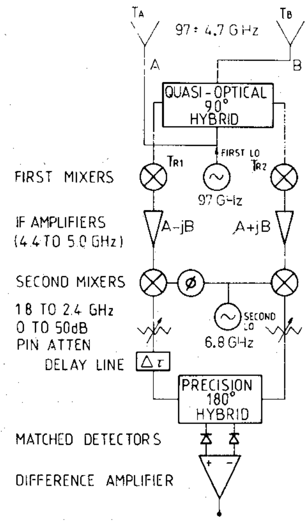

Fig. 1. Radiometer block diagram. The two inputs at temperatures of T_A and T_B are split and combined in a quasi-optical hybrid. After mixing at 97 GHz, they are amplified and phase shifted to optimize the response. A precision 180° hybrid and matched detectors are used to "multiply" the two IF signals.

The amplitude of the incoming signal in the upper sideband (USB) and in the lower sideband (LSB) is proportional to the square root of the input temperature. In the following equations, the unprimed quantities are from the USB and primed quantities from the LSB. The complex conjugate is represented by the symbol (*). The input temperatures in the signal and reference beams are denoted by T_A and T_B, respectively, and the two receiver temperatures are T_{R1} and T_{R2}. The signal amplitudes are A and A' and the reference amplitudes B and B', in the two sidebands. The amplitudes for the receiver noise in channels 1 and 2 are R_1 and R'_1 and R_2 and R'_2, respectively. These amplitudes are related to the temperatures by

$$T_A = A\times A^* + (A')\times(A')^* \tag{2a}$$

$$T_B = B\times B^* + (B')\times(B')^* \tag{2b}$$

$$T_{R1} = R_1\times R^*_1 + (R'_1)\times(R'_1)^* \tag{2c}$$

$$T_{R2} = R_2\times R^*_2 + (R'_2)\times(R'_2)^*. \tag{2d}$$

In general, the 90° beam-splitter hybrid does not split the signals equally but has amplitudes of ρ for reflection and τ for transmission, which are assumed to be the same for both sidebands. Depending on how the LO is injected, the continuous comparison radiometer can be realized with a 180 or 90° input hybrid. After going through the quasi-optical hybrid, the signal amplitudes are

$$V_1 = j\exp(j\omega_{LO}t)\{1 + (\rho A - j\tau B + R_1)\exp(j\omega_1 t) + (\rho A' - j\tau B' + R'_1)\exp(-j\omega_1 t)\} \tag{3a}$$

$$V_2 = \exp(j\omega_{LO}t)\{1 + (\tau A + j\rho B + R_2)\exp(j\omega_1 t) + (\tau A' + j\rho B' + R'_2)\exp(-j\omega_1 t)\} \tag{3b}$$

where j is the square root of (-1), ω_{LO} the angular frequency of the 97-GHz LO, ω_1 the first IF angular frequency, and t is time. The signal level of the 97-GHz LO is represented by the first term in the expressions for V_1 and V_2. It is arbitrarily set to 1 to show the phase of the LO. The second and third terms are the upper and lower sidebands, respectively.

After double-sideband mixing with the 97-GHz LO, gain at the first IF and LSB mixing from 4.7 (ω_1) to 2.1 GHz (ω_2) with a 6.8-GHz second LO, the voltages are

$$V_3 = \exp(j\phi)G_1\{(\rho A - j\tau B + R_1)\exp(-j\omega_2 t) + (\rho A' - j\tau B' + R'_1)\exp(j\omega_2 t)\} \tag{4a}$$

$$V_4 = G_2\{(\tau A + j\rho B + R_2)\exp(-j\omega_2 t) + (\tau A' + j\rho B' + R'_2)\exp(j\omega_2 t)\} \tag{4b}$$

where the term $\exp(j\phi)$ is the relative phase shift introduced by the 6.8-GHz phase shifter and G_1 and G_2 are the voltage gains in the two channels.

At the output of the precision 180° IF hybrid, the voltages are

$$V_5 = (V_3 + V_4)\sqrt{2} \tag{5a}$$

$$V_6 = (V_3 - V_4)\sqrt{2}. \tag{5b}$$

The detected power is obtained by multiplying V_5 and V_6 by their complex conjugates and low-pass filtering to remove harmonics of the IF components. Cross products such as $A\times B$ and $R_1\times R_2$ will average out to zero when the inputs are uncorrelated and there is no correlated noise in the two receiver temperatures. In the following discussion, K and $K(1-\delta)$ represent the product of the detector sensitivities and difference amplifier gains for the two detected outputs, where the magnitude of (δ) is less than 0.05. In this case, the voltage, of the two outputs are

$$V_7 = [K/2]\{T_A[(\rho G_1)^2 + (\tau G_2)^2 + (2\rho\tau G_1G_2)\cos(\phi)] + T_B[(\tau G_1)^2 + (\rho G_2)^2 - (2\rho\tau G_1G_2)\cos(\phi)] + T_{R1}(G_1)^2 + T_{R2}(G_2)^2 \tag{6a}$$

$$V_8 = [K(1-\delta)/2] \cdot \{T_A[(\rho G_1)^2 + (\tau G_2)^2 - (2\rho\tau G_1G_2)\cos(\phi)] + T_B[(\tau G_1)^2 + (\rho G_2)^2 + (2\rho\tau G_1G_2)\cos(\phi)] + T_{R1}(G_1)^2 + T_{R2}(G_2)^2\}. \tag{6b}$$

Then, the output of the radiometer is the difference of V_7 and V_8

$$V_{out} = K\{[(2\rho\tau G_1G_2)(T_A - T_B)\cos(\phi)] + (\delta/2)\{T_A[(\rho G_1)^2 + (\tau G_2)^2] + T_B[(\tau G_1)^2 + (\rho G_2)^2)] + T_{R1}(G_1)^2 + T_{R2}(G_2)^2\}. \tag{7}$$

The quartz beam splitter splits the signal with 54 percent of the incident power being reflected and 46 percent transmitted. This gives values for ρ and τ of 0.750 and 0.667, so that ($2\rho\tau$) equals 0.996. When the two IF gains are equal, as is the case for normal operation, the system output is proportional to the input temperature difference plus a fractional offset term due to the detector imbalance. In this case, the output is given by

$$V_{\text{out}} = (KG_1G_2)\{(T_A - T_B)\cos(\phi) + (\delta)[(T_A + T_B)/2 + (T_{R1} + T_{R2})/2]\}. \quad (8)$$

With the precision IF hybrid and careful matching of the detectors, δ can be reduced to less than 0.001. This will give an offset on the order of 0.5 K, which can be measured by cycling through the second LO phase ϕ, or can be subtracted out by observing the source alternately in beam A and beam B.

III. Front-End System

The two input beams are 51 mm apart at the Cassegrain focus of a 13.7-m-diam telescope with a f/d ratio of 4.0. This gives two 1.0′-diam beams which are 3.3′apart in azimuth on the sky. This close beam separation was chosen to optimize the cancellation of atmospheric effects. A wider beam separation could be designed if broader sources were to be mapped. The inputs are linearly polarized with the two polarizations 110° apart.

As is schematically shown in Fig. 2, the front-end portion of the system consists of the input optics, the scalar feeds, the cryogenic millimeter mixers, and the IF amplifiers. All of these are integrated into the cryogenics Dewar which is 250×300×400 mm in size. The top and bottom covers have O-ring and RF shielding grooves. This design has given a very reliable system. The cooling to 15 and 77 K is done with a CTI 350CP closed-cycle helium refrigerator. A 0.8-mm-thick aluminum shield is attached to the 77 K station of the refrigerator to minimize the thermal radiation loading on the 15 K components. Part of this heat shield is lined with a microwave absorber to act as a black body at 77 K for the LO signal which is not coupled into the mixers and to terminate any reflections and spillover in the optics at 77 K.

As is described in detail in the next section, the optics take the beams at the Cassegrain focus of the antenna, expand them so that the LO can be injected, and combine the two beams in the quasi-optical 90° hybrid. The beams are then refocused to match into the scalar feeds.

The 97.3-GHz LO is provided by a Gunn-diode oscillator having 10 mW of power. The output of the oscillator is isolated and attenuated before going through a waveguide vacuum feedthrough. Inside the Dewar, the LO is coupled into the optics with a rectangular horn, a rexolite focusing lens, and two flat mirrors.

Double-sideband mixing is done in a pair of Schottky-diode millimeter mixers which are cooled to 15 K. The mixers have been developed at the FCRAO and have broad-band RF filters and noncontacting backshorts. They utilize GaAs diodes which have a low doping of 3×10^{16} cm^{-3} to give an optimum performance when cryogenically cooled [8], [9]. The mixer blocks are machined from OFHC copper to minimize their RF losses and have a linear taper from full- to 1/4-height waveguide. The RF filter has been designed to present a short to the diode at 97 GHz and is reactive at the second harmonic of the LO to minimize

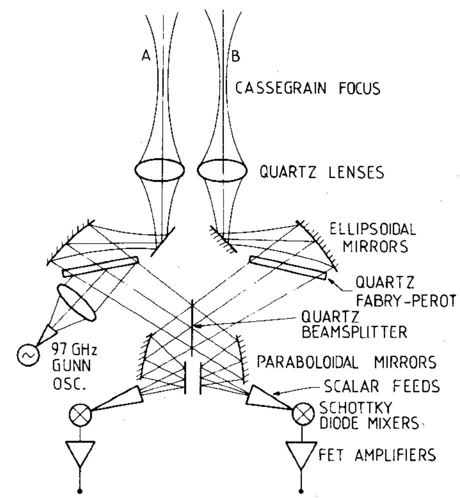

Fig. 2. Radiometer optics diagram. The symmetrical system uses fused-silica lenses to focus the inputs from the Cassegrain focus into the cryogenic Dewar. A thin sheet of fused-silica acts as a 90° hybrid. Then the 97-GHz LO is injected via a dielectric Fabry–Perot and the beams are refocused into the millimeter mixers.

conversion to higher harmonics. The noncontacting backshort has also been especially designed [10] to be a short circuit at 97 GHz and a pure reactance at 194 GHz. The backshort position was optimized at room temperature and locked into place with a setscrew before cooling the system to 15 K. The whisker length has been optimized since its length tunes the mixer response versus the input frequency [8].

Cooled circulators and FET amplifiers give an IF noise temperature of 25–30 K over the 4.4–5.0-GHz band. Each IF chain consists of an input isolator [12], FET amplifier [13], and output isolator at 20 K, providing a net gain of 11 dB. A second FET with 12 dB more gain is mounted on the 77 K station of the closed-cycle helium refrigerator. The circulators and amplifiers which were made at the FCRAO are followed by commercial amplifiers at 300 K, which are mounted within the vacuum chamber. Their 55 dB of gain gives a net RF to IF gain of 80 dB before the signals leave the RF-shielded Dewar. These signals are then processed as discussed in Section V.

IV. Optics

The input optics to the radiometer serve multiple purposes. They

1) illuminate the subreflector of the 14-m-diam telescope with a 12-dB edge taper,
2) inject the local oscillator power at 97.3 GHz,
3) combine the input beams in such a way as to create a quasi-optical 90° hybrid for the two sidebands at 93 and 102 GHz.

The optics block diagram is shown in Fig. 2. The photograph in Fig. 3 shows the front end with the vacuum Dewar removed. This view shows the optics after the fused-silica lenses. Fig. 4 shows the beam propagation in one plane so that the various optical elements and the Gaussian beam can be accurately displayed. In the actual

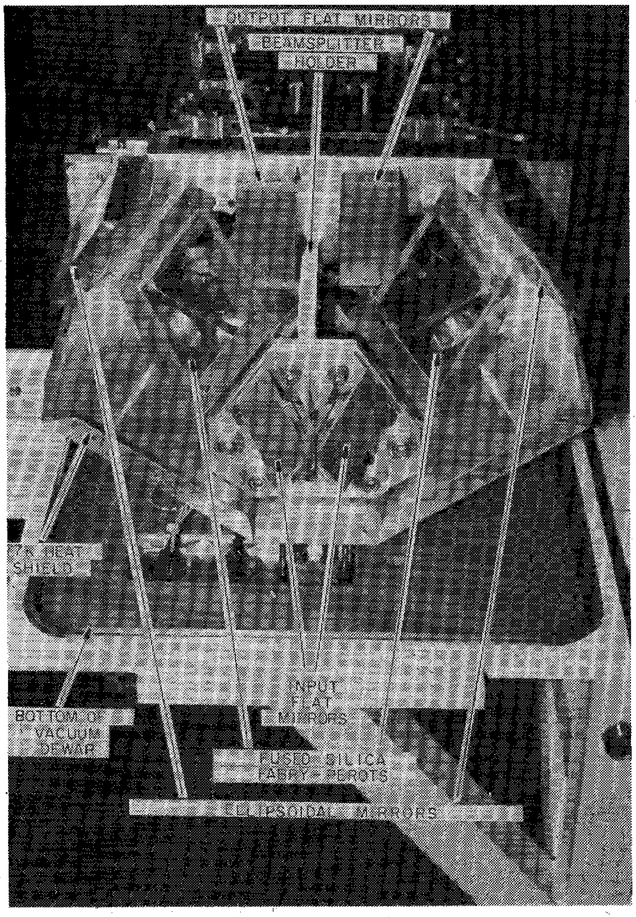

Fig. 3. Front-view of front-end system. The input flat mirrors at the lower center divert the two input beams up to the ellipsoidal mirrors at the upper left and right of the optics. The dielectric Fabry–Perots are just below the ellipsoidal mirrors. The local oscillator is injected from behind the left Fabry–Perot. The beam-splitter holder is indicated. The paraboloidal mirrors are behind the input flat mirrors. The scalar feed horns and the mixers are behind the output flat mirrors.

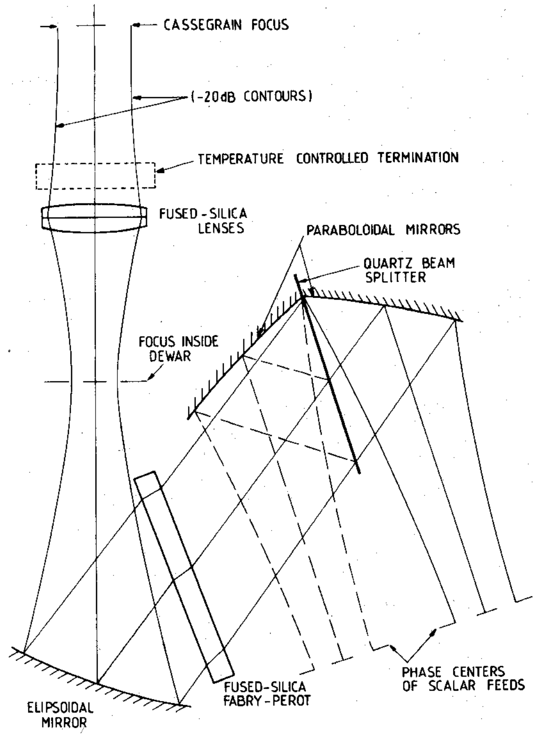

Fig. 4. Gaussian beam propagation within optics. The beam is traced through the optics at the −20-dB contour level. All of the elements are shown in one plane even though the beam path is folded in the system for compactness.

receiver, the optical path is folded with two sets of flat mirrors to condense the optics into a volume of 8l. This is 3×10^5 cubic wavelengths at 97.3 GHz and is a reasonable minimum size for a two-channel system with LO injection and a beam splitter.

The input optics comprise both LO injection and a 90° hybrid beam combiner. Their operation is explained with reference to Fig. 2. The input signals are beams A and B. The LO power is injected into beam A only by using a dielectric Fabrey–Perot interferometer (FPI), which has a signal transmission of >95 percent and a LO reflectivity of 30 percent. Then beams A and B are split in a dielectric beam splitter which produces approximately equal amplitudes in reflection and transmission. A general property of a lossless symmetric beam splitter is that the reflected and transmitted waves differ in phase by 90°. Assuming all input phases are 0 (this phase is arbitrary), the outputs of this splitter are

$$A/2+jB/2+\mathrm{LO}/2$$
$$j(A/2-jB/2+\mathrm{LO}/2).$$

This method of injecting the LO before the splitter has several advantages critical to the simplicity and stability of the system. One is that no additional power splitter is needed to divide the LO for the mixers, and only one FPI plate is needed. However, a second FPI plate is included in the optics to preserve the system symmetry. More important is the advantage in terms of phase stability. In this method, no dimensional variations before the beam-splitter hybrid have any effect on phase stability. After the beam splitter, the two paths to the mixer must be equal and stable in length only to within a small fraction of the IF wavelength (63 mm). In a system in which the LO is independently split, phase equality of the two LO paths is critical, as is any phase drift in the LO injection filter.

The only disadvantage of this approach is that any AM noise on the LO, offset from the carrier, is mixed down to 4.7 GHz and appears as a difference signal. This will be attenuated by the rejection of the FPI plate, which is about 8 dB. In the case of this radiometer, the imbalance term is less than 2 K and can be measured in the calibration procedure. Should stability of this noise be a concern, it can be further reduced by a cavity filter in the LO waveguide.

Table I summarizes the parameters of the Gaussian beams at various points in the optics. Included are the beam diameter at a −20-dB power level, the characteristic length Z_c for the beam, the distance to the next element in the optics and the focal lengths of the lenses, and two sets of mirrors. This system was designed to truncate the Gaussian beams at the −20-dB level to minimize the volume of the system with a loss of about 2 percent at each truncation. Normally, one would design the system to

TABLE I
GAUSSIAN BEAM PARAMETERS WITHIN OPTICS

Description	Beam Diameter (-20 dB)	Z_c	Distance To Next Element	Focal Length
Cassegrain Focus	28 mm	87 mm	72 mm	---
Fused Silica Lenses	36	---	63	57 mm
Focus Inside Dewar	18	36	115	---
Ellipsoidal Mirror	60	---	180	106
Paraboloidal Mirror	52	291	121	157
Scalar Feed	24	65	---	---

Given at various positions within the optics system are the beam diameter at the -20-dB level, the confocal parameter Z_c, the spacing between elements, and the focal lengths for the lenses and mirrors in the system.

truncate at -30 dB or a lower contour with a resultant increase in the volume of the system by a factor of 2.

The acceptance angle of the radiometer optics is such that the Cassegrain secondary edge illumination is 12 dB down from the axial power. The focus of the telescope is located 72 mm in front of the Dewar windows. As is illustrated in Fig. 4 and noted in Table I, the beam begins to diverge again, passes through the calibration wheel, and into the Dewar through the quartz (fused silica) lenses. Each lens is made up of a pair of plano-convex lenses placed back to back, with 0.5-mm-thick polyethylene antireflection coatings fused to the curved surfaces. The resulting lens has a focal length of 57 mm. This lens brings the beam to a second focus 63 mm inside the Dewar.

The beam then diverges to fill the ellipsoidal mirrors. The ellipsoidal mirrors are sections of an ellipse of revolution such that the distances to the two foci of the ellipse are 150 and 650 mm, and the angle subtended by the two foci is 37°. The distances of 150 and 650 mm are the radii of curvature of the input and output Gaussian beams at the reflecting surface. The radius of curvature of a Gaussian beam at a distance Z from the beam waist is [11]

$$R(Z)=Z\left[1+(Z_c/Z)^2\right] \tag{9}$$

where Z_c is given in Table I. The output beam is approximately plane parallel, as indicated by the large Z_c of 291 mm, for minimum loss in the dielectric Fabry–Perot.

The 8.6-mm-thick fused-silica dielectric slab is used as a tuned filter to inject the 97.3-GHz LO into the two mixers. The plates are tilted at 32° with respect to normal incidence. This slab transmits the two sidebands with very low loss and reflects about 30 percent of the power at the LO frequency [14], [15]. Only one of these plates is actually used for LO injection; the other is necessary to preserve system balance. The theoretical walkoff loss is less than 5 percent [16], with a measured limit of less than 10 percent.

The functioning of the offset paraboloidal mirrors is best explained by considering the 24-mm beam-waist diameter at the -20-dB contour generated by the scalar feedhorns. The Gaussian beam from the scalar feed has a radius of curvature of 156 mm at the paraboloidal mirror, and the focus of the parabola of revolution is at the center of curvature of the incident wave. This causes an approximately plane-parallel beam to be developed between the paraboloidal and ellipsoidal mirrors. The beam waist is located near the surface of the paraboloidal mirror.

The ellipsoidal and paraboloidal mirrors were machined on a conventional milling machine [17] from aluminum and then hand polished. These mirrors were then rigidly attached to a 6-mm-thick aluminum plate. The only adjustments in the optics were the exact focal position of the scalar feeds and the position and angle of the flat mirrors which are just behind the input lenses.

V. IF PROCESSING

The two 4.4–5.0-GHz IF signals from the front-end system are processed with a computer-controlled IF system to automatically calibrate and optimize the radiometer and to scale the difference output. As was shown in Fig. 1, both channels are converted from 4.7 to 2.1 GHz with the same 6.8-GHz LO. The 6.8-GHz LO is split with a zero-degree power splitter. One of the LO lines to the double-balanced mixers has a digitally controlled 6-bit phase shifter with a 0–354° range and a 5.6° resolution. The LO lines to the two mixers have isolators to minimize coupling between the two channels via the common LO system. The output of each mixer has a linear-phase bandpass filter with a 600-MHz 1-dB bandwidth, centered at 2.1 GHz. These are followed by 0–55-dB p-i-n attenuators which are also under computer control. Their normal attenuation is about 10 dB to minimize their phase shift versus attenuation. The last amplifiers are set to give a output power level of -20 dBm in the 600-MHz wide band. The two IF chains have selected pairs of filters and amplifiers with matched phase and delay responses. Any residual delay is compensated by a delay line or specially made cables. The power level at the output of each IF chain is monitored to set the p-i-n attenuators and to calibrate the receiver temperature as described in the next section.

The two IF signals are combined in a precision IF hybrid with 45 dB of isolation between ports. The low-barrier Schottky detector diodes have an output load resistor chosen for best square-law response at -20 dBm. Once the detectors are temperature stabilized to ± 1°C, the system output is nulled by changing the sensitivity of one of the two detectors. This part of the system has the largest effect on the system balance.

The difference amplifier has a RC time constant of 2.7 ms. Its output is sampled at a 1-KHz rate with a 12-bit analog-to-digital converter. The IF and dc gains are adjusted so that the output range is ± 250 K, giving a resolution of 0.12 K. This is to be compared with the output noise of >0.28 K in 2.7 ms. The output noise fluctuation has been derived by Faris [1]

$$\Delta T_{\mathrm{rms}}=\left[2/(\tau_t \mathrm{BW})\right]^{1/2}\left[(T_{R1}+T_{R2})/2+(T_A+T_B)/2\right] \cdot\left[\sin(\pi \mathrm{BW}\tau_d)/(\pi \mathrm{BW}\tau_d)\right]\cos(\omega_2\tau_d+\phi) \tag{10}$$

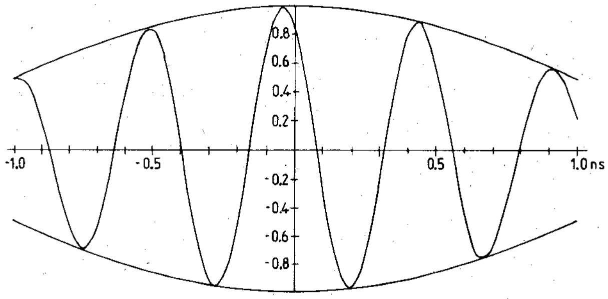

Fig. 5. Phase and delay response of system. The broad envelope is determined by the $\sin(X)/X$ response due to the final IF bandwidth of 600 MHz. The rapid cosinusoidal variation within this envelope is due to delay differences between the two IF's and can be optimized with the LO phase shifter.

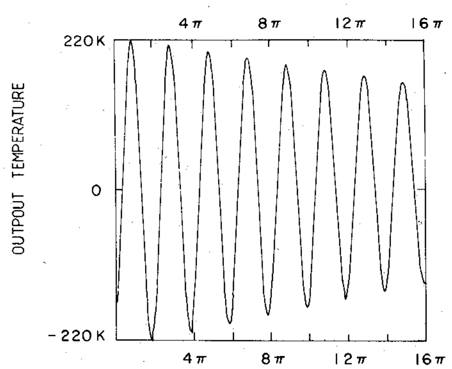

Fig. 6. System response versus LO phase and IF gain. The system output for an input temperature difference of 220 K is shown versus LO phase. The system was calibrated for the first cycle of 0 to 2 π. One of the IF gains was reduced in 0.4-dB steps in each subsequent 2 π interval.

where BW is the 600-MHz IF bandwidth, τ_i the output integration time, τ_d the time-delay difference between the two channels, ω_2 the second IF angular frequency, and ϕ the relative LO phase. The effect of the last two terms of (10) is illustrated in Fig. 5 for delay errors up to 1 ns. The envelope is the $\sin(x)/(x)$ response due to the 600-MHz IF bandwidth. In the actual system, the delay was adjusted so that the sensitivity loss from this effect was less than 5 percent. The cosine term is then automatically optimized during the calibration procedure to be greater than 0.99 by adjusting ϕ. For average receiver and input temperatures of 250 and 77 K, the expected rms is 0.019 K in 1 s. The measured output fluctuations are 0.033 K rms with the fraction due to the receiver noise being 0.025 K.

The output response is given by (8) and is shown in Fig. 6 for one input terminated at room temperature (295 K) and the other at liquid nitrogen temperature (77 K). The output temperature scale is determined by the 218-K temperature difference and was set with the initial IF gains (G_1 and G_2). As the LO phase (ϕ of Fig. 1 and (1) and (8)) is varied over 2π, the output varies between ± 220 K because of the cosinusoidal dependence on ϕ. The following cycles of 2π had G_1 (see (8)) reduced in 0.4-dB steps. Thus, the system does not require balanced IF gains since changing the gain 3 dB only changes the calibration by a factor of 0.7. In this case, the imbalance δ (8) was about 0.03, so

TABLE II
CALIBRATION WHEEL POSITIONS

Position	Channel A	Channel B
1	318 K	318 K
2	Sky	Sky
3	Sky	323 K
4	323 K	313 K
5	313 K	Sky

The inputs to channels A and B are shown for the 5 different positions. The inputs either look at the sky or at temperature-controlled terminations.

that the cycles are only approximately symmetrical about zero.

VI. Calibration Procedure

An essential part of the radiometer is the integral calibration system. This allows the output to be scaled into temperature, and also the receiver temperature and the sky contribution to the system temperature to be measured. This is accomplished with four temperature-controlled loads which are cast from Emerson–Cuming CR-117. Two of these loads are stabilized within 0.1°C of each other at 45°C (318 K). The other pair are maintained at 313 K and 323 K to give a known temperature difference for calibrating the output of the whole radiometer.

The calibration wheel has five different position angles which are under computer control. Table II lists the terminations which are observed by inputs A and B for each of the five positions of the wheel. Position 1 gives a balanced input with two loads at 318 K to calibrate the zero of the difference output. Position 2 has two open ports for normal observing. Position 3 has an open on input A and a load at 323 K on input B. Position 4 has a load at 323 K on input A and 313 K on input B to calibrate the output temperature scale. Position 5 has a load at 313 K on input A and an open on input B.

The amplitude and phase of the sinusoidal response of the system output is found with a multiple linear regression routine in the MODACS computer. Offsets in the detectors and dc amplifiers are measured by setting the p-i-n attenuators to their maximum attenuation of 55 dB. Position 5, with its large temperature difference between the sky at a typical temperature of 100 K and the 313 K load, is used to find the phase corresponding to the peak response from the difference amplifier. The amplitudes $[A(3), A(4), A(5)]$ of the IF output versus LO phase at wheel Positions 3, 4, and 5 are used to measure the sky temperature from the known temperature difference of 10 K

$$T_{\rm SKY} = (313+323)/2 - 10[A(3)+A(5)]/[2A(4)]. \tag{11}$$

The 6.8-GHz LO phase shifter (ϕ of Fig. 1 and (1) and (8)) is then commanded to the phase found at wheel Position 5 and the outputs of power detectors in each IF chain, just before the 180° hybrid, are measured in wheel Positions 1 and 2. This gives a Y-factor for each channel with the hot and cold temperatures supplied by the 318 K loads and the sky, respectively. The system temperature measured for each channel in this manner is 250 K outside the Dewar including the window and optics losses.

VII. Conclusions

A continuous comparison radiometer has been implemented at a wavelength of 3 mm having a sensitivity of 0.025 K in 1 s. Its major features include

1) an integral calibration system to determine the temperature scale, sky contribution, and receiver temperature,
2) a dielectric Fabry–Perot interferometer used for LO injection,
3) quasioptical 90° input hybrid,
4) optics integrated into the vacuum and cryogenics system to minimize the system noise temperature and the system volume of the front end,
5) cryogenic mixers and FET amplifiers with DSB reciever temperatures of less than 250 K,
6) separate delay and phase optimization,
7) precision IF hybrid and matched detectors,
8) a computer system to optimize and calibrate the radiometer.

Acknowledgment

The authors acknowledge the help of the entire staff of the Five College Radio Astronomy Observatory in making this project successful. The Five College Radio Astronomy Observatory is operated with the permission of the Metropolitan District Commission, Commonwealth of Massachusetts. This is contribution number 591 of the Five College Astronomy Department. One of the authors (C.R.P.) thanks the Institut de Radio Astronomie Millimetrique, Grenoble, France, where part of the writing was done, and the University of Massachusetts for a professional improvement leave.

References

[1] J. J. Faris, "Sensitivity of a correlation radiometer," *J. Res. Nat. Bur. Stand., Sect. 71C (Engr. and Instr.)*, pp. 153–170, Apr.–June 1967.

[2] C. G. T. Haslam, W. E. Wilson, D. A. Graham, and G. C. Hunt, "A further 408 MHz survey of the northern sky," *Astron. Astrophys. Suppl.*, vol. 13, pp. 359–394, 1974.

[3] S. Wongsowijoto and A. Schmidt, "Ein 3-Kanal-Empfanger fur 11cm-Messungen mit dem 100-m-Teleskop," Kleinheubacher Berichte, Ed. Fermeldetechnisches Zentralamt: Darmstadt 25, 1982, pp. 371–376.

[4] G. T. Haslam, U. Klein, C. J. Salter, H. Stoffel, W. E. Wilson, M. N. Cleary, D. J. Cooke, and P. Thomasson, "A 408 MHz all-sky continuum survey," *Astron. Astrophys.*, vol. 100, pp. 209–219, 1981.

[5] J. M. Payne, "Switching subreflector for millimeter wave radio astronomy," *Rev. Sci. Instrum.*, vol. 47, pp. 222–223, Feb. 1976.

[6] R. H. Dicke, "The measurement of thermal radiation at microwave frequencies," *Rev. Sci. Instrum.*, vol. 17, pp. 268–275, 1946.

[7] P. F. Goldsmith, "Quasioptical feed system for radioastronomical observations at millimeter wavelengths," *Bell. Syst. Tech. J.*, vol. 56, p. 1483, 1977.

[8] A. V. Raisanen, "Experimental studies on cooled millimeter wave mixers," *Acta Polytechnica Scandinavica*, Elect. Eng. series no. 46, Oct. 1980.

[9] J. L. R. Marrero, "75–115 GHz cryogenic heterodyne receiver," M.S. thesis, Univ. of Massachusetts, Sept. 1981.

[10] M. K. Brewer and A. V. Raisanen, "Dual-harmonic noncontacting millimeter waveguide backshorts: Theory, design, and test," *IEEE Trans. Microwave Theory Tech.*, vol. MTT-30, pp. 708–714, May 1982.

[11] A. V. Raisanen, N. R. Erickson, J. L. R. Marrero, P. F. Goldsmith, and C. R. Predmore, "An ultra low-noise schottky mixer receiver at 80-120 GHz," in *Infrared and Millimeter-wave Conf. Proc.*, Dec. 1981, pp. W3.8–9.

[12] A. Wu, "Assembly and testing procedure for a cryogenically-cooled 5 GHz circulator," National Radio Astronomy Observatory Electronics Division Int. Rep. 207, July 1980.

[13] S. Weinreb, "Low-noise cooled GASFET amplifiers," *IEEE Trans. Microwave Theory Tech.*, vol. MTT-28, pp. 1041–54, Oct. 1980.

[14] P. F. Goldsmith, "Quasi-optical techniques at millimeter and submillimeter wavelengths," in *Infrared and Millimeter Waves*, vol. 6, K. J. Button, Ed. New York: Academic, pp. 277–343, 1982.

[15] P. F. Goldsmith, "Diffraction loss in dielectric-filled Fabry–Perot interferometers," *IEEE Trans. Microwave Theory Tech.*, vol. MTT-30, pp. 820–823, May 1982.

[16] P. F. Goldsmith, "Quasioptics in millimeterwave systems," in *12th Eur. Microwave Conf. Proc.*, Sept. 1982, pp. 16–24.

[17] N. R. Erickson, "Off-axis mirrors made using a conventional milling machine," *Appl. Opt.*, vol. 18, pp. 956–957, Apr. 1, 1979.

C. Read Predmore (M'73) received the B.S. degree in physics from Virginia Polytechnic Institute, Blacksburg, in 1967, and the Ph.D. degree in physics from Rice University, Houston, TX, in 1971.

From 1971 to 1973, he was an Assistant Professor in the Department of Space Physics and Astronomy at Rice University, where he continued his work on radio astronomy and initiated a submillimeter laser project. In 1972, he joined the National Radio Astronomy Observatory, where he worked on the development and design of the TE_{01} transmission system for the Very-Large-Array radio telescope. Since 1975, he has been at the University of Massachusetts, Amherst, where he is doing research and development for the millimeter-wave telescope of the Five College Radio Astronomy Observatory. In 1982/83, he spent a year's leave at the Institut de Radio Astronomie Millimetrique in Grenoble, France, and the Helsinki University of Technology.

Dr. Predmore is a member of the American Astronomical Society and the URSI.

Neal R. Erickson was born in Peoria, IL, on January 3, 1949. He received the B.S. degree from the California Institute of Technology, Pasadena, in 1970, and the Ph.D. degree from the University of California, Berkeley, in 1979.

Since 1979, he has been working as a Postdoctoral Associate at the Five College Radio Astronomy Observatory, University of Massachusetts, Amherst. He is involved in the development of receivers, quasi-optical devices, and frequency multipliers for the near-millimeter and submillimeter regions, and is also active in the field of millimeter and submillimeter radio astronomy.

G. Richard Huguenin (M'82) received the B.S. degree in physics from M.I.T. and the Ph.D. from Harvard University.

He was a member of the Harvard faculty until he moved to the University of Massachusetts to found the Five College Radio Astronomy Observatory. Under his directorship, the observatory grew steadily until today it is one of the top university radio observatories in the U.S. In January 1982, he founded MilliTech Corporation, whose primary business is the marketing, development, manufacture, and sales of millimeter and submillimeter components and subassemblies. These components are used in research, communications, and instrumentation applications by companies and research facilities all over the world.

Paul F. Goldsmith (M'75) received the A.B. and Ph.D. degrees from the University of California, Berkeley, in 1969 and 1975, respectively.

After two years as a Member of the Technical Staff at Bell Laboratories, he joined the faculty of the University of Massachusetts, Amherst. He is presently Associate Professor of Physics and Astronomy and acting Director of the Five College Radio Astronomy Observatory. He is Vice President for engineering at the MilliTech Corporation, founded in 1981.

Short Papers

Active Stabilization of Crystal Oscillator FM Noise at UHF Using a Dielectric Resonator

ANTHONY G. MANN

Abstract —**A low-noise 600-MHz crystal oscillator circuit is described. It uses a dielectric oscillator as the dispersive element of a discriminator in an active frequency stabilization loop which reduces the near-carrier FM noise. The innovation in the circuit is an essentially noiseless active carrier suppression loop, which allows maximum utilization of a low-noise RF amplifier to reduce the discriminator threshold ($\Delta f_{\rm rms}$) to 2.5×10^{-5} Hz in a 1-Hz bandwidth. The FM noise 1 kHz from the carrier was reduced by 44 dB to this threshold, equivalent to a phase-noise spectral density of -152 dBc/Hz.**

I. Introduction

A 600-MHz oscillator with very low near-carrier FM noise is required for an ultra-sensitive superconducting re-entrant cavity accelerometer [1]. Since the accelerometer is used to measure the displacement at a specific audio frequency (nominally 1 kHz), we require extremely low FM noise 1 kHz from the carrier. The best commercially available crystal oscillators and synthesizers have FM noise of 10^{-3} Hz in a 1-Hz band 1 kHz from the carrier. The lowest noise solid-state source reported to date [2], developed by Alley and Wang, has FM noise (normalized to 600 MHz) of 1.8×10^{-4} Hz in a 1-Hz bandwidth. Discriminators, however, can detect much lower levels of FM noise because, all else being equal (available power and resonator Q), their noise temperature can be that of a low-noise RF amplifier (typically 440 K) if adequate carrier suppression is available. Hence, the motivation for building an active frequency stabilization circuit around a state-of-the-art voltage-controlled crystal oscillator (VCXO) and a discriminator based on a high Q, temperature-stable dielectric resonator which can handle high power. The work described here is, therefore, to some extent based on the work of Alley and Wang, and is largely experimental.

This work was supported in part by the National Science Foundation under Grant PHY-81-07388.

Manuscript received March 26, 1984; revised August 1, 1984.

The author is with the Department of Physics and Astronomy, Louisiana State University, Baton Rouge, LA 70803.

II. The Dielectric Resonator

The heart of the frequency discriminator is the dielectric resonator, which at 600 MHz requires a disk size near the technological limit of fabrication. Three discs, each 8.89 cm in diameter and 2.54 cm thick, were fabricated from Trans-Tech D-8514 material, a zirconium/tin titanate having a relative dielectric constant of 37.7 and a frequency-temperature coefficient of $+3$ ppm/°C. For Q measurement, the discs were supported on a plastic beaker inside a large aluminum enclosure. The unloaded Q's of the $TE_{01\delta}$ modes for stacks of 1, 2, and 3 discs (mode frequencies 675, 560, and 514 MHz, respectively) were in the range 23 000 to 26 000.

The prototype resonator shown in Fig. 1 uses 3 discs stacked one on top of the other. This stack simply rests on a ground plane inside a cylindrical aluminum container. This configuration is not optimum because the proximity of the walls, especially the lower ground plane, decreases the unloaded Q to 10 000 and overcompensates for the frequency-temperature coefficient of the discs. The resonator frequency-temperature coefficient was measured at -2 ppm/°C (over 25°C to 100°C) with the coupling loop negligibly small. Since the loop diameter necessary for critical coupling perturbs the resonant frequency by as much as 100 ppm, variations in loop geometry contribute to the resonator frequency stability. Fortuitiously, thermal expansion of the teflon dielectric in the 3-cm section of 0.085-in (2.1 mm) semi-rigid coaxial cable supporting the loop modifies the net frequency-temperature coefficient to about -1 ppm/°C near room temperature. Tuning is accomplished with a micrometer-driven aluminum piston which has sufficient resolution to obtain carrier nulls as deep as 43 dB when the coupling is made critical. However, due to micrometer backlash and thermal drift of the coupling coefficient, the resonator carrier suppression is conservatively set to about 25 dB.

0018-9480/85/0100-0051$01.00